Available online at www.sciencedirect.com

SciVerse ScienceDirect

Ceramics International 38 (2012) 4765–4770

CERAMICS INTERNATIONAL

www.elsevier.com/locate/ceramint

Influence of sintering temperature on energy storage properties of $BaTiO_3$–$(Sr_{1-1.5x}Bi_x)$ TiO_3 ceramics

Qian Zhang, Yong Zhang *, Xiangrong Wang, Tao Ma, Zongbao Yuan

Beijing Fine Ceramics Laboratory, State Key Laboratory of New Ceramics and Fine Processing, Institute of Nuclear and New Energy Technology, Tsinghua University, Beijing 100084, PR China

Received 29 September 2011; received in revised form 13 February 2012; accepted 22 February 2012
Available online 3 March 2012

Abstract

The effect of sintering temperature on microstructure, dielectric properties and energy storage properties of $BaTiO_3$–$(Sr_{1-1.5x}Bi_x)TiO_3$ ($x = 0.09$) (BT–SBT) ceramics was investigated. The sintering temperature has pronounced influence on the grain size, shrinkage, and dielectric properties of the BT–SBT ceramics. With increasing sintering temperature, the dielectric constant increases largely. However, the increasing tendency of the dielectric breakdown strength (BDS) is less noticeable but become more evident with the consideration of Weibull modulus. For the BT-SBT ceramics, the unreleased energy density decreases and the electric field stability of the energy storage efficiency enhances with the increase of sintering temperature.

© 2012 Elsevier Ltd and Techna Group S.r.l. All rights reserved.

Keywords: A. Sintering; C. Dielectric properties; D. $BaTiO_3$ and titanates; Energy storage property

1. Introduction

With the rapid depletion of fossil fuels and increasingly worsened environmental pollution caused by vast fossil-fuel consumption, there is high demand to make efficient use of energy and to seek renewable and clean energy sources such as solar energy and wind energy that can substitute fossil fuels to enable the sustainable development. Energy storage, as an intermediate step to the versatile, clean, and efficient uses of energy, receives tremendous attention and research interests. The conversion and storage of energy are closely related to energy storage materials [1]. Therefore, the development of energy storage techniques can be largely attributed to the innovation and advancement of energy storage materials.

Up to now, many efforts, such as using compositions with Curie temperatures well below the operating temperature [2], optimization of the microstructure [3], sintering and crystallization [4], addition or doping in the glass ceramics [5–7] and so on, have focused on improving the energy storage properties of ceramics so as to attain high energy storage density capacitors. Since the energy storage density is related to the product of applied electric field squared and dielectric constant [8], improvements in dielectric properties, especially dielectric constant and breakdown strength, have a more pronounced effect on the energy storage density.

The earlier works have reported that sintering temperature had significant influences on the densification, microstructure [9] and dielectric properties [10,11] of ceramics. Such behavior was also found in $(Ba,Sr)TiO_3$ glass-ceramics [12] and suggested that the density, grain size, dielectric constant and tunability increase with increasing sintering temperature. Much attention has been paid to the sintering temperature dependence of the microstructure and dielectric properties of $Ba_{1-x}Sr_xTiO_3$ ceramics. However, only a few studies have been reported on the relation between the energy storage properties and the sintering temperature, especially in the $BaTiO_3$–$(Sr_{1-1.5x}Bi_x)$-$)TiO_3$ (BT–SBT) ceramics which integrate the high dielectric constant of $BaTiO_3$ ceramics near Curie temperature and the good dielectric properties of $(Sr_{1-1.5x}Bi_x)TiO_3$ ceramics, such as low Curie temperature, low dissipation factor, and good electric-field tunability [13]. In this paper, the BT–SBT ceramics were prepared by a solid state reaction method. The microstructure, dielectric properties and polarization

* Corresponding author. Tel.: +86 10 80194055; fax: +86 10 89796022.
E-mail address: yzhang@tsinghua.edu.cn (Y. Zhang).

0272-8842/$36.00 © 2012 Elsevier Ltd and Techna Group S.r.l. All rights reserved.
doi:10.1016/j.ceramint.2012.02.064

hysteresis loops of the BT–SBT ceramics as a function of sintering temperature were investigated and the relationship between these observations and the variation of energy storage properties was revealed.

2. Experimental procedure

2.1. Synthesis

Conventional solid state reaction method was applied in preparing the BT–SBT samples from analytical reagent grade powders of $SrCO_3$, Bi_2O_3, TiO_2, MnO_2, SnO_2 (AR, Beijing Sinopharm chemical reagent Co. Ltd., Beijing, China) and commercial-grade hydrothermal $BaTiO_3$ (Guoteng Co. Ltd., Shandong, China). The $SrCO_3$, Bi_2O_3, and TiO_2 powders were ball milled with alcohol and zirconia balls in polyethylene jars for 6 h. After drying, the mixture was calcined at 1090 °C for 2 h to synthesize $(Sr_{1-1.5x}Bi_x)TiO_3$ ($x = 0.09$) (SBT) followed by re-milling. The appropriate amounts of $BaTiO_3$, MnO_2, and SnO_2 powders were mixed with the SBT powder to synthesize $BaTiO_3$–$(Sr_{1-1.5x}Bi_x)$-$)TiO_3$ (BT–SBT) phase. Then the BT–SBT powder was mixed with a small amount of polyvinyl acetate (PVA) binder and uniaxially pressed to form disk-shaped pellets with 10 mm in diameter and 1–2 mm in thickness under a pressure of 40 MPa. After binder burnout, the pressed disks were sintered in a temperature range from 1160 °C to 1220 °C for 2 h in a closed crucible.

2.2. Characterization

The microstructure observation and analysis of the fracture surfaces of the ceramic specimens were performed with a scanning electron microscope (SEM: FEI Qunanta 200 FEG). To determine the dielectric properties, silver paste was coated to form electrodes on both sides of the parallel surfaces, and subsequently fired at 550 °C for 30 min. The temperature dependence of dielectric constant and loss was determined at frequencies between 1 kHz and 1 MHz by means of a LCR meter (HP4284) interfaced with a computer, while the specimens were heated at a constant rate of 2 °C/min. For dielectric breakdown strength (BDS) testing, the circular specimens with 1–1.5 mm in thickness were tested in silicon oil to prevent arcing. The BDS measurements were carried out with a high voltage source HF5013 K (Changzhou Huiyou Electronics Co. Ltd., China). A DC voltage ramp of about 1 kV/s was applied to the specimens until the dielectric breakdown occurred. At least 8 specimens were used for each sintering temperature during BDS testing. The polarization-electric field (*P*-*E*) hysteresis loops were measured at room temperature by a Sawyer–Tower capacitive voltage divider in a computerized measuring system. All electric fields were supplied by a high voltage power supply (Trek 609-B, NY, USA) driven by a frequency generator (HP33220A, CA, USA). The electric field was applied from 1 to 6 kV/mm under 1 Hz during measurement.

3. Results and discussion

3.1. Microstructure

SEM micrographs of the fracture surface of the BT–SBT ceramics as a function of sintering temperature are shown in Fig. 1. The microstructures of the BT–SBT ceramics varied with the sintering temperature. As the sintering temperature increased, the average grain size increased, and the porosity decreased. At 1220 °C, sufficient grain growth occurred, resulting in a homogenous grain size distribution with a little amount of pores being trapped in the microstructure. This leads to the largest shrinkage rate and the highest density for the BT–SBT ceramic specimens sintered at 1220 °C. The average grain size and shrinkage as a function of sintering temperature for the BT–SBT ceramics are illustrated in Table 1.

3.2. Dielectric properties

As shown in Fig. 2, we employ the Weibull distribution to perform the statistical analysis for the BDS of the BT–SBT ceramics sintered at various temperatures. The reasonable values of the BDS can be described in the form of following equation:

$$\ln\ln\left(\frac{1}{1-P_i}\right) = m\ln(E_i - E_u) - \ln\left(\frac{(E_b)^m}{N}\right) \quad (1)$$

where P_i is the probability for dielectric breakdown, N is the specimen space, E_i is the resultant BDS, E_u is the BDS when the probability for electric breakdown is zero, E_b is the mean BDS, and m is the Weibull modulus which represents the credence of the statistic results [14]. When $m \leq 1$, it indicates that the model is improper for the failure analysis, and the breakdown distribution does not obey the Weibull function. And when $m > 1$, it indicates that the failure could be analyzed by the Weibull model [15]. The greater the m is, the more reliable the model would be [16].

The specimens are arranged in ascending order of BDS values so that $E_1 \leq E_2 \leq \ldots E_i \ldots \leq E_n$. The estimator of P_i for the ith strength is expressed as

$$P_i = \frac{i}{1+N} \quad (2)$$

The Weibull plots of the BDS of the BT–SBT ceramics sintered at different temperatures are shown in Fig. 2. It was observed that with all these m values being bigger than 1, the BDS are more reliable. In addition, it is seen that all of the plots show relatively good linearity, indicating that the scattering in each data set can be expressed by the two parameter Weibull distribution function. By Eq. (1), the average dielectric breakdown strength E_b is obtained by the slope m and the intercept $-m\ln(E_b)$.

The results of the change in the BDS as a function of sintering temperature for the BT–SBT ceramics are shown in Fig. 3. The increasing tendency of the BDS is not clearly seen but become more evident with the consideration of Weibull

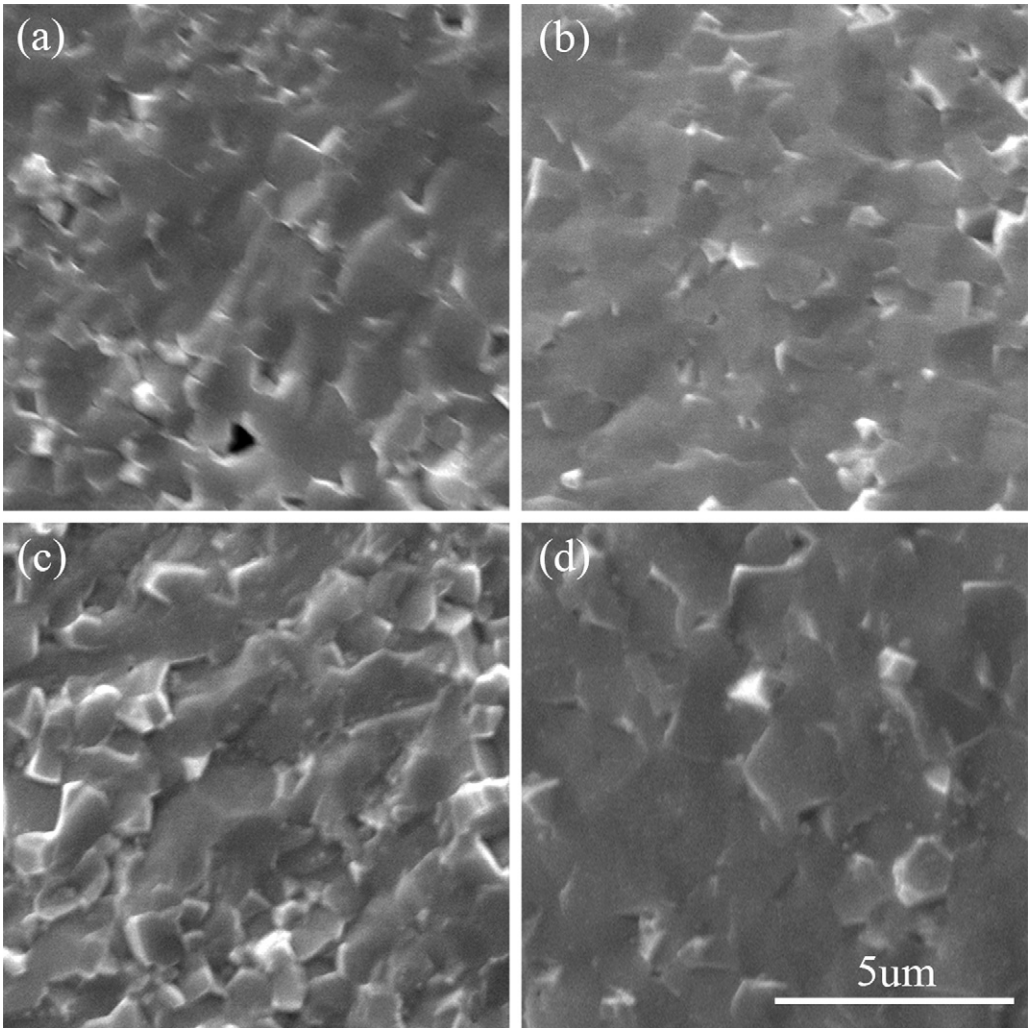

Fig. 1. SEM micrographs of the fracture surface of the BT–SBT ceramics specimens sintered at. (a) 1160 °C, (b) 1180 °C, (c) 1200 °C, (d) 1220 °C.

modulus. The anomalous BDS of the BT–SBT ceramics sintered at 1160 °C might be attributed in partly to the relatively lower value of the Weibull modulus *m* as shown in Fig. 2. It is noteworthy that both the BDS and shrinkage rate of the BT–SBT ceramics increase with the increase of the sintering temperature up to 1220 °C. The BDS of ceramics depends on several factors, such as porosity [5,17], grain size [18], and interfacial polarization [19] and so on. In this work, the porosity of the samples was reduced with increasing sintering temperature, which is believed to be the main reason for the improvement of the BDS. On the other hand, the more homogeneous microstructure also contributes to the improvement of the BDS.

Table 1
The grain size and shrinkage rate of the BT–SBT ceramics sintered at various sintering temperatures.

Sintering temperature (°C)	Grain size (μm)	Shrinkage rate (%)
1160	0.97	12.19
1180	1.03	12.20
1200	1.05	12.60
1220	1.29	12.76

The variation of dielectric constant and dielectric loss with sintering temperature for the BT–SBT ceramics is shown in Fig. 4. The measurements were carried out in a temperature range from −55 to 120 °C at 1 kHz. The dielectric constant increases as the sintering temperature increases over the entire measuring temperature range. The dielectric constant maximum at the

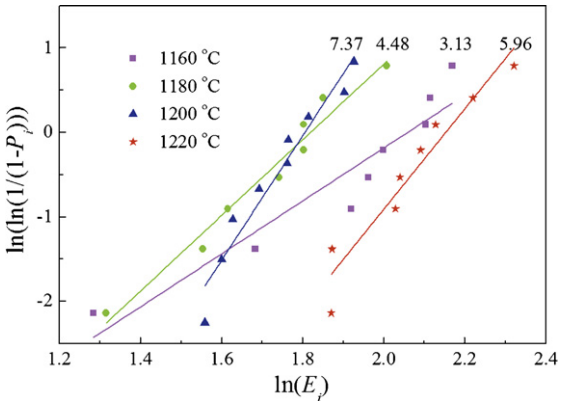

Fig. 2. Weibull plots of the dielectric breakdown strength of the BT–SBT ceramics with different sintering temperatures.

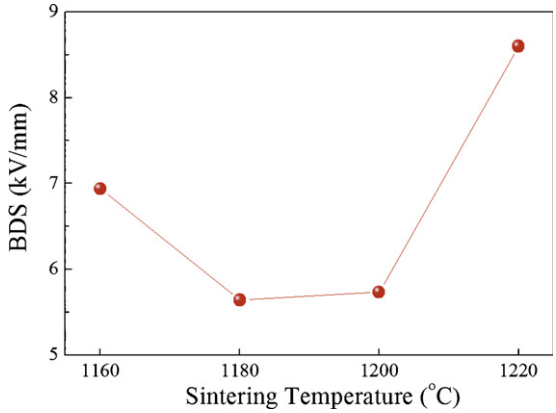

Fig. 3. The BDS as a function of sintering temperature for the BT–SBT ceramics.

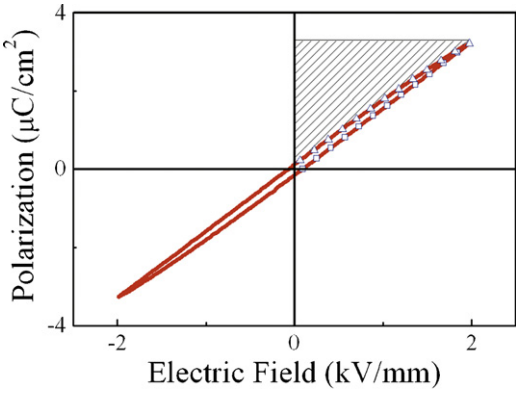

Fig. 5. Schematic illustration of *P-E* hysteresis loop for the BT–SBT ceramics.

transition temperature (T_c) systematically increases as the sintering temperature increases for the BT–SBT ceramics. Close inspection of the transition temperature reveals that there is small shift in T_c with sintering temperature. The increase in the dielectric constant maximum with increasing sintering temperature was related to the increase in the grain size as shown in Fig. 1. Additionally, with increasing sintering temperature, the dielectric loss increases at the ferroelectric state, while it does not change obviously at the paraelectric state. Furthermore, the dielectric loss for the BT–SBT ceramics was less than 0.01 in the temperature range from 0 to 120 °C. This is promising as most applications for capacitors require low loss and good thermal stability.

As mentioned above, the general trends of the BT–SBT ceramics indicate an increase in both the dielectric constant and the BDS with increasing sintering temperature. This is consistent with the measurement results of the shrinkage rate for the BT–SBT ceramics.

3.3. Energy storage properties

The energy storage behavior of the BT–SBT ceramics with different sintering temperatures was investigated in terms of the polarization-electric field (*P-E*) hysteresis loops. Fig. 5 shows a typical loop for the BT–SBT ceramics. The charged energy density (J_c) of a dielectric material is equal to integral of the area enclosed by charge curve and *y*-axis. And the discharged energy density (J_d) is equal to integral of the area enclosed by discharge curve and *y*-axis [8,20].

The charged and discharged energy densities of the BT–SBT ceramics were calculated from the *P-E* hysteresis loops measured at room temperature. It was shown that both the charged and discharged energy densities increase with the increase of measuring electric field. However, they are not very sensitive to the sintering temperature. Though the dielectric constant and the BDS increased with the increase of sintering temperature, the energy density only slightly changed. This result was partially due to the relatively low polarization as shown in Table 2. And the highest charged energy density of 0.3 J/cm^3 was obtained under a high electric field (6 kV/mm). Furthermore, the relation between the discharged energy density and the electric field could be well simulated by quadratic polynomial, $J_d = aE^2 + bE + c$, as listed in Table 3. And the results showed that J_d increased with the square of E, which suggests that, by improving the ceramic microstructure to raise the E_b, a much higher energy density can be achieved.

As a parameter to evaluate the energy storage property, the unreleased energy density is as important as the discharged energy density. The unreleased energy densities as a function of electric field are presented in Fig. 6. All the samples exhibited the unreleased energy densities of less than 0.07 J/cm^3 at the electric field of 6 kV/mm. With the increase of the sintering temperature, the unreleased energy densities of the BT–SBT ceramics decrease over the entire electric field range. This observation can be explained in terms of the increase in grain

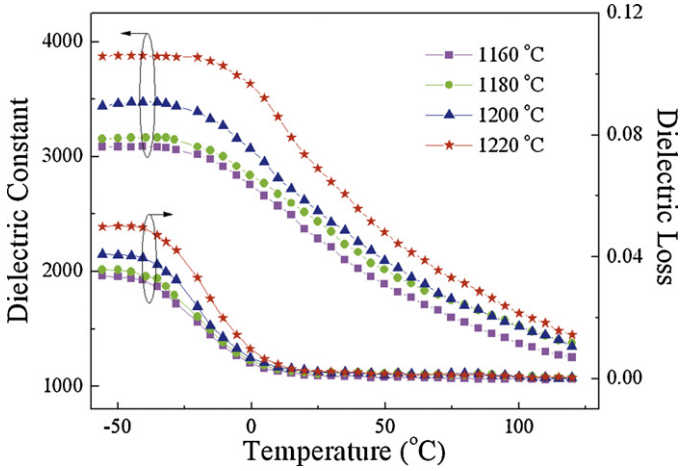

Fig. 4. Temperature dependence of the dielectric constant and dielectric loss at 1 kHz for the. BT–SBT ceramic specimens sintered at different sintering temperatures.

Table 2
The coercive electric field (E_c) and remanent polarization (P_r) for the samples with different sintering temperatures.

Sintering temperature (°C)	1160	1180	1200	1220
E_c (kV/mm)	0.34	0.26	0.28	0.28
P_r (μC/cm^2)	0.69	0.42	0.46	0.40
P_{max} (μC/cm^2)	7.75	7.82	7.33	7.35

Table 3
The values of quadratic polynomial coefficient and intercept for the samples sintered at different sintering temperatures and the corresponding adjusted R^2.

Sintering temperature (°C)	Coefficient		Intercept	Adjusted R^2
	a	*b*	*c*	
1160	0.0047	0.0098	−0.0097	0.9981
1180	0.0056	0.0074	−0.0068	0.9999
1200	0.0050	0.0077	−0.0069	0.9999
1220	0.0052	0.0071	−0.0069	0.9999

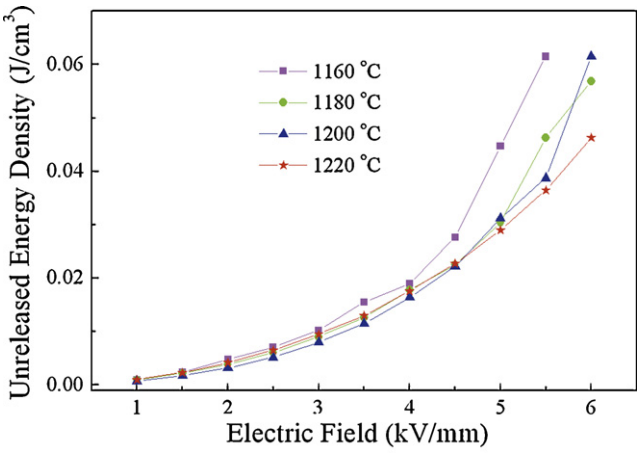

Fig. 6. The unreleased energy density versus electric field for the BT–SBT ceramics sintered at different sintering temperatures.

sizes. It is believed that the unreleased energy density is related with Maxwell–Wagner polarization. This interfacial polarization of coarse-grained ceramics is much lower than that of fine-grained ceramics. In addition, these results agree well with the values of coercive electric field (E_c) and remanent polarization (P_r) shown in Table 2.

Fig. 7 illustrates the values of energy storage efficiency (J_d/J_c) [4] for the BT–SBT ceramics sintered at different temperatures. Interestingly, the energy storage efficiency of the BT–SBT ceramics was up to 90%. The energy storage efficiency of the BT–SBT ceramics decreases with increasing electric field, which originates from a dramatic increase in the unreleased energy density (Fig. 6). The energy storage efficiency has a complex dependence on the sintering temperature. The BT–SBT ceramics sintered at 1220 °C exhibit a steady dependence of the energy storage efficiency on the electric field. A slight change appears between 1 and 6 kV/mm. Such electric field stability of the energy storage efficiency increases with the increase of the sintering temperature. Less variation of the energy storage efficiency is benefit for the utilization of ceramic capacitors in a wider field range.

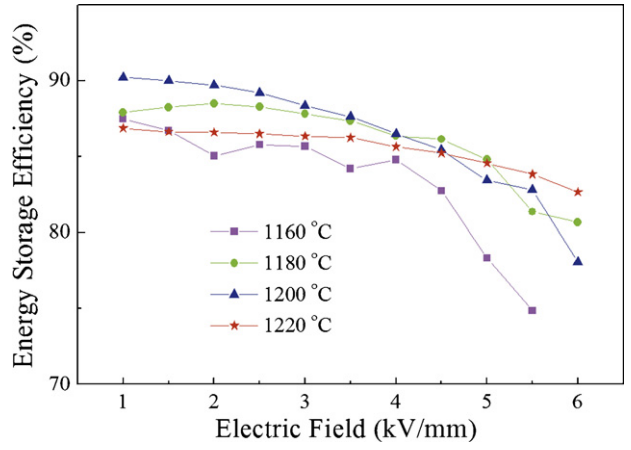

Fig. 7. The energy storage efficiency as a function of electric field for the BT–SBT ceramics with different sintering temperatures.

4. Conclusions

The BT–SBT ceramics were fabricated by a solid state reaction process with various sintering temperatures. As the sintering temperature increases, both the average grain size and the shrinkage rate of the BT–SBT ceramics increase. The major effect of the sintering temperature on the dielectric characteristics of the BT–SBT ceramics is the increase in dielectric constant. Also, by taking the Weibull modulus into consideration, the dielectric breakdown strength of the BT–SBT ceramics was found to be increased with the increase of the sintering temperature. The unreleased energy density decreases as the sintering temperature is increased. Moreover, a steady dependence of the energy storage efficiency on the electric field was observed for the ceramic samples sintered at 1220 °C. It is believed that the larger grain size results in the improvement of the energy storage behavior for the BT–SBT ceramics.

Acknowledgments

This work was supported by the National Natural Science Foundation of China (Grant No. 50977049) and Tsinghua University Initiative Scientific Research Program. Technical help by D. H. Hao is recognized.

References

[1] C. Liu, F. Li, L.P. Ma, H.M. Cheng, Advanced material for energy storage, Adv. Mater. 22 (2010) E28–E62.
[2] N.H. Fletcher, A.D. Hilton, B.W. Ricketts, Optimization of energy storage density in ceramic capacitors, J. Phys. D: Appl. Phys. 29 (1996) 253–258.
[3] H. Ogihara, C.A. Randall, S.T. Mckinstry, High-energy density capacitors utilizing 0.7 $BaTiO_3$–0.3$BiScO_3$ ceramics, J. Am. Ceram. Soc. 92 (2009) 1719–1724.
[4] Y. Zhang, J.J. Huang, T. Ma, X.R. Wang, C.S. Deng, X.M. Dai, Sintering temperature dependence of energy-storage properties in (Ba,Sr)TiO_3 glass-ceramics, J. Am. Ceram. Soc. 94 (2011) 1805–1810.
[5] Q.M. Zhang, L. Wang, J. Luo, Q. Tang, J. Du, Improved energy storage density in barium strontium titanate by addition of BaO–SiO_2–B_2O_3 glass, J. Am. Ceram. Soc. 92 (2009) 1871–1873.
[6] E.P. Gorzkowski, M.J. Pan, B. Bender, C.C.M. Wu, Glass-ceramics of barium strontium titanate for high energy density capacitors, J. Electroceram. 18 (2007) 269–276.
[7] G.X. Dong, S.W. Ma, J. Du, J.D. Cui, Dielectric properties and energy storage density in ZnO-doped $Ba_{0.3}Sr_{0.7}TiO_3$ ceramics, Ceram. Int. 35 (2009) 2069–2075.

[8] I. Burn, D.M. Smyth, Energy storage in ceramic dielectrics, J. Mater. Sci. 7 (1972) 339–343.
[9] M. Mazaheri, A.M. Zahedi, S.K. Sadrnezhaad, Two-step sintering of nanocrystalline ZnO compacts: effect of temperature on densification and grain Growth, J. Am. Ceram. Soc. 91 (2008) 56–63.
[10] L. Szymczak, Z. Ujma, J. Handerek, J. Kapusta, Sintering effects on dielectric properties of (Ba,Sr)TiO_3 ceramics, Ceram. Int. 30 (2004) 1003–1008.
[11] B. Su, J.E. Holmes, B.L. Cheng, T.W. Button, Processing effects on the microstructure and dielectric properties of barium strontium titanate (BST) ceramics, J. Electroceram. 9 (2002) 111–116.
[12] B. Zhang, X. Yao, L.Y. Zhang, J.W. Zhai, Effect of sintering condition on the dielectric properties of (Ba,Sr)TiO_3 glass-ceramic, Ceram. Int. 30 (2004) 1773–1776.
[13] Y. Zhi, A. Chen, R. Guo, A.S. Bhalla, Dielectric properties and tunability of (Sr,Bi)TiO_3 with MgO additive, Mater. Lett. 57 (2003) 2927–2931.
[14] W. Weibull, A statistical distribution function of wide applicability, J. Appl. Mech. 18 (1951) 293–302.
[15] J. Luo, J. Du, Q. Tang, C.H. Mao, Lead sodium niobate glass-ceramic dielectrics and internal electrode structure for high energy storage density capacitors, IEEE Trans. Electron. Dev. 55 (2008) 3549–3554.
[16] Y. Wang, Y.C. Chan, Z.L. Gui, D.P. Webb, L.T. Li, Application of Weibull distribution analysis to the dielectric failure of multilayer ceramic capacitors, Mater. Sci. Eng. B 47 (1997) 197–203.
[17] G. Robert, M.C. Thomas, Dielectric breakdown of porous ceramics, J. Appl. Phys. 30 (1959) 1650–1653.
[18] A. Young, G. Hilmas, S.C. Zhang, R.W. Schwartz, Effect of liquid-phase sintering on the breakdown strength of barium titanate, J. Am. Ceram. Soc. 90 (2007) 1504–1510.
[19] J.J. Huang, Y. Zhang, T. Ma, H.T. Li, L.W. Zhang, Correlation between dielectric breakdown strength and interface polarization in barium strontium titanate glass ceramics, Appl. Phys. Lett. 96 (2010) 042902.
[20] S. Chao, F. Dogan, $BaTiO_3$–$SrTiO_3$ layered dielectrics for energy storage, Mater. Lett. 65 (2011) 978–981.